

**Supplemental information**

**Dynamic interplay between IL-1 and WNT pathways  
in regulating dermal adipocyte lineage cells  
during skin development and wound regeneration**

**Lixiang Sun, Xiaowei Zhang, Shuai Wu, Youxi Liu, Christian F. Guerrero-Juarez, Wenjie Liu, Jinwen Huang, Qian Yao, Meimei Yin, Jiacheng Li, Raul Ramos, Yanhang Liao, Rundong Wu, Tian Xia, Xinyuan Zhang, Yichun Yang, Fengwu Li, Shujun Heng, Wenlu Zhang, Minggang Yang, Chi-Meng Tzeng, Chao Ji, Maksim V. Plikus, Richard L. Gallo, and Ling-juan Zhang**

State 1	State 2		State 3					
perifollicular (C2,5,9)	PAP (C7)	RET (C3)	AP /pAd (C4)	pAd /eAd (C8)	HI- pAd (C10)	Areg (C6)	HI-AP (C11)	
<i>CD24<sup>hi</sup></i>	<i>Entpd1</i>	<i>Ptgfr</i>	<i>Cebpb</i>	<i>Pparg</i>	<i>Agt</i>	<i>Mgp</i>	<i>Wnt2</i>	
<i>Alpl</i>	<i>Lrig1</i>	<i>Cyp4b1</i>	<i>Lgr5</i>	<i>Fabp4</i>	<i>Icam1</i>	<i>Fmo2</i>	<i>Smpd3</i>	
<i>Sox2</i>	<i>Grem1</i>	<i>Sfrp2</i>	<i>Icam1</i>	<i>Plin1</i>	<i>Lpl</i>	<i>F3</i>	<i>Cd34</i>	
<i>Lef1</i>	<i>Lum<sup>hi</sup></i>	<i>Col1a1</i>	<i>Plin2</i>	<i>Plin2</i>	<i>Plin2</i>	<i>Sfrp4</i>	<i>Col14a1</i>	
<i>Inhba</i>				<i>Lpl</i>			<i>Fn1<sup>hi</sup></i>	
<i>Col23a1</i>				<i>Agt</i>				
<i>Trps1</i>	high	med	low	low	low	low	low	low
<i>Dlk1</i>	low	low	med	med	med	high	high	high
<i>Dpp4</i>	low	med	low	low	low	low	low	high
<i>Ly6a</i>	low	low	low	med	med	med	med	high

**Table S1. Key marker genes for indicated dFB cell clusters in neonatal mouse skin.**

**Table S2. List of Abbreviations:**

Abbreviations	Definitions
AP	Adipocyte progenitor
AD	Adipocyte progenitor
APM	Arrector pili muscle
AREG	Adipogenesis regulators
dFB	Dermal fibroblast
DP	Dermal papilla
DS	Dermal sheath
dWAT	Dermal white adipose tissue
EC	Endothelial cell
ECM	Extracellular matrix
FACS	Fluorescence activated cell sorting
GT	Grannule tissue
HF	Hair follicle
HB	Hair bulb
HI-AP	Hypodermal interstitial adipocyte progenitor
IHC	Immunohistochemistry
KC	Keratinocyte
KC-IFE	Keratinocyte-interfollicular epidermis
LV	Lymphatic vessel
myoFB	Myo-fibroblast
NB	Neonatal fibroblast
pAd	Pre-adipocyte
PAP	Papillary
PHA	Phalloidin
RET	Reticular
RET-AP	Reticular-adipocyte progenitor
scRNA-seq	Single-cell RNA sequencing
TAM	Tamoxifen
TFs	Transcriptional factors
tSNE	t-distributed stochastic neighbor embedding
UMAP	Uniform manifold approximation and projection
VSMC	Vascular smooth muscle cell
w.d.	Wound day

**Table S3 List of protein and gene symbols:**

Proteins	Protein symbols	Gene symbols
Actin Alpha 2	ACTA2	<i>Acta2</i>
Adiponectin	ADIPOQ	<i>Adipoq</i>
RAC-alpha serine/threonine-protein kinase	AKT	<i>Akt</i>
Alkaline phosphatase, tissue-nonspecific isozyme	ALPL	<i>Alpl</i>
Patatin-like phospholipase domain-containing protein 2	ATGL	<i>Pnpla2</i>
Axin-2	AXIN2	<i>Axin2</i>
Cathelicidin antimicrobial peptide	CAMP	<i>Camp</i>
Signal transducer CD24	CD24	<i>Cd24</i>
T-cell surface glycoprotein CD3	CD3	<i>Cd3</i>
Hematopoietic progenitor cell antigen CD34	CD34	<i>Cd34</i>
Platelet glycoprotein 4	CD36	<i>Cd36</i>
Receptor-type tyrosine-protein phosphatase C	CD45	<i>Ptprc</i>
CCAAT/enhancer-binding protein beta	CEBPB	<i>Cebpb</i>
Collagen	COL	<i>Col</i>
Cellular retinoic acid-binding protein 1	CRABP1	<i>Crabp1</i>
Cyclic AMP-responsive element-binding protein 1	CREB	<i>Creb1</i>
CCN family member 2	CTGF	<i>Ccn2</i>
C-X-C motif chemokine	CXCL	<i>Cxcl</i>
Decorin	DCN	<i>Dcn</i>
Protein delta homolog 1	DLK1	<i>Dlk1</i>
Dipeptidyl peptidase 4	DPP4	<i>Dpp4</i>
Ectonucleoside triphosphate diphosphohydrolase 1	ENTPD1	<i>Entpd1</i>
Mitogen-activated protein kinase	ERK	<i>Mapk</i>
Coagulation Factor III	F3	<i>F3</i>
Dimethylaniline monooxygenase [N-oxide-forming] 2	FMO2	<i>Fmo2</i>
Fibronectin	FN1	<i fn1<="" i=""></i>
Green fluorescent protein	GFP	<i>Gfp</i>
Glycogen synthase kinase-3	GSK3	<i>Gsk3</i>
Intercellular adhesion molecule 1	ICAM1	<i>Icam1</i>
Interleukin-1	IL1	<i>Il1</i>
Interleukin-1 receptor type 1	IL1R1	<i>Il1r1</i>
Proliferation marker protein Ki-67	Ki67	<i>Mki67</i>
Keratin	KRT	<i>Krt</i>
Lymphoid enhancer-binding factor 1	LEF1	<i>Lef1</i>
Leucine-rich repeat-containing G-protein coupled receptor 5	LGR5	<i>Lgr5</i>
Lipoprotein lipase	LPL	<i>Lpl</i>

Leucine-rich repeats and immunoglobulin-like domains protein 1	LRIG1	<i>Lrig1</i>
Lumican	LUM	<i>Lum</i>
Lymphocyte antigen 6A-2/6E-1	LY6A	<i>Ly6a</i>
Lysozyme C-2	LYZ2	<i>Lyz2</i>
Matrix Gla protein	MGP	<i>Mgp</i>
Myosin regulatory light chain 2, skeletal muscle isoform	MYLPF	<i>Mylpf</i>
Myogenin	MYOG	<i>Myog</i>
Nuclear factor NF-kappa-B p105 subunit	NFKB	<i>Nfkb</i>
Protein naked cuticle homolog 2	NKD2	<i>Nkd2</i>
Proliferating cell nuclear antigen	PCNA	<i>Pcna</i>
Platelet-derived growth factor receptor alpha	PDGFRA	<i>Pdgfra</i>
Perilipin	PLIN	<i>Plin</i>
Peroxisome proliferator-activated receptor gamma	PPARG	<i>Pparg</i>
Transcription factor SOX-2	SOX2	<i>Sox2</i>
Sterol regulatory element-binding protein 1	SREBF1	<i>Srebf1</i>
Transgelin	TAGLN	<i>Tagln</i>
Transforming growth factor beta	TGFB	<i>Tgfb</i>
Transforming growth factor-beta-induced protein ig-h3	TGFBI	<i>Tgfbi</i>
Thy-1 membrane glycoprotein	THY1	<i>Thy1</i>
Wnt Family Member 2	WNT2	<i>Wnt2</i>

**Table S4. List of primers used for RT-qPCR of mouse genes:**

<b>Gene</b>	<b>Strand</b>	<b>Primer sequence</b>
<b><i>Tbp</i></b>	Forward	CCTTGACCCTTCACCAATGAC
	Reverse	ACAGCCAAGATTCACGGTAGA
<b><i>Camp</i></b>	Forward	CAAGGAACAGGGGGTGG
	Reverse	TCCGGCTGAGGTACAAGTTT
<b><i>Dlk1</i></b>	Forward	TGGCTGGGACGGGAAATTC
	Reverse	CACGCAAGTTCCATTGTTGGC
<b><i>Col1a1</i></b>	Forward	GCTCCTCTTAGGGGCCACT
	Reverse	ATTGGGGACCCTTAGGCCAT
<b><i>Thy1</i></b>	Forward	CCTTACCCTAGCCAACCTCAC
	Reverse	AGGATGTGTTCTGAACCAGC
<b><i>Pdgfra</i></b>	Forward	ATGAGAGTGAGATCGAAGGCA
	Reverse	CGGCAAGGTATGATGGCAGAG
<b><i>Ly6a</i></b>	Forward	GAGGCAGCAGTTATTGTGGAT
	Reverse	CGTTGACCTTAGTACCCAGGA
<b><i>Pparg1</i></b>	Forward	AAGAAGCGGTGAACCACTGA
	Reverse	GGAATGCGAGTGGTCTTCCA
<b><i>Adipoq</i></b>	Forward	CACACCAGGCCGTGATGGCA
	Reverse	GAAGCCCCGTGGCCCTTCAG
<b><i>Fabp4</i></b>	Forward	GTGGGAGTGGGCTTTGCCACA
	Reverse	CACCAGGGCCCCGCCATCTA
<b><i>Cd24a</i></b>	Forward	TTCTGGCACTGCTCCTACC
	Reverse	GCGTTACTTGGATTTGGGGAA
<b><i>Il6</i></b>	Forward	ACAAAGCCAGAGTCCTTCAGAGAGA
	Reverse	AGCCACTCCTTCTGTGACTCCAG
<b><i>Acta2</i></b>	Forward	GGCACCCTGAACCCTAAGG
	Reverse	ACAATACCAGTTGTACGTCCAGA
<b><i>Spp1</i></b>	Forward	TCTCCTTGCGCCACAGAATG
	Reverse	GGCTTTCATTGGAATTGCTTGG
<b><i>Dpp4</i></b>	Forward	TATGCCAGTTTAACGACACAG
	Reverse	ACAGTTGGATTCACAGCTCCT
<b><i>Sox2</i></b>	Forward	GCGGAGTGGAACCTTTGTCC
	Reverse	CGGGAAGCGTGTACTTATCCTT
<b><i>Alpl</i></b>	Forward	CCAACTCTTTTGTGCCAGAGA
	Reverse	GGCTACATTGGTGTGAGCTTTT
<b><i>Inhba</i></b>	Forward	TGTGGGTAAAGTGGGGGAGA
	Reverse	CACGCTCCACTACTGACAGG
<b><i>Lef1</i></b>	Forward	AACGAGTCCGAAATCATCCCA
	Reverse	GCCAGAGTAACTGGAGTAGGA
<b><i>Crabp1</i></b>	Forward	CAGCAGCGAGAATTTTCGACGA
	Reverse	CGCACAGTAGTGGATGTCTTGA

<b>Lrig1</b>	Forward	TTGAGGACTTGACGAATCTGC
	Reverse	CTTGTTGTGCTGCAAAAAGAGAG
<b>Col23a1</b>	Forward	CCCATCTGAGTGCATCTGTC
	Reverse	CTTGCCGTCCAGACCTAGAG
<b>Col14a1</b>	Forward	TTTGGCGGCTGCTTGTTC
	Reverse	CGTTTTGTGCAGTGTCTG
<b>Lgr5</b>	Forward	CCTACTCGAAGACTTACCCAGT
	Reverse	GCATTGGGGTGAATGATAGCA
<b>Cebpb</b>	Forward	CAAGAGCCGCGACAAGGCCA
	Reverse	CTCGCGACAGCTGCTCCACC
<b>Cd36</b>	Forward	AGATGACGTGGCAAAGAACAG
	Reverse	CCTTGGCTAGATAACGAACTCTG
<b>Lpl</b>	Forward	GGGAGTTTGGCTCCAGAGTTT
	Reverse	TGTGTCTTCAGGGGTCCTTAG
<b>Lipe</b>	Forward	AGGATCGAAGAACCGCAGTC
	Reverse	GTCTTCTGCGAGTGTCACCA
<b>Smpd3</b>	Forward	TCATGGACGTGGCCTATCAC
	Reverse	GCAGGCGATGTACCCAACAA
<b>Wnt2</b>	Forward	CTCGGTGGAATCTGGCTCTG
	Reverse	CACATTGTCACACATCACCT
<b>Il1r1</b>	Forward	GTGCTACTGGGGCTCATTGT
	Reverse	GGAGTAAGAGGACACTTGCGAAT
<b>Il4ra</b>	Forward	TCTGCATCCCGTTGTTTTGC
	Reverse	GCACCTGTGCATCCTGAATG
<b>Cxcl12</b>	Forward	TGCATCAGTGACGGTAAACCA
	Reverse	TTCTTCAGCCGTGCAACAATC
<b>Cxcl5</b>	Forward	TGCCCTACGGTGAAGTCATA
	Reverse	TGCATTCCGCTTAGCTTTCTTT
<b>Axin2</b>	Forward	CGAGTGTGAGATCCACGGAA
	Reverse	GGACATGGAATCGTCGGTCA
<b>F3</b>	Forward	GCCATTTACAAACGCCCAA
	Reverse	GCAGGGTGAGGAATGTACCA
<b>Atgl</b>	Forward	AACGCCACTCACATCTACGG
	Reverse	CAATCAGCAGGCAGGGTCTT
<b>Tnc</b>	Forward	CAGCTACCGACGGGATCTTC
	Reverse	TTCCGGTTCAGCTTCTGTGG
<b>Il1b</b>	Forward	GAAATGCCACCTTTTGACAGTG
	Reverse	TGGATGCTCTCATCAGGACAG
<b>Ly6g</b>	Forward	GACTTCCTGCAACACAACCTACC
	Reverse	ACAGCATTACCAGTGATCTCAGT
<b>Nkd2</b>	Forward	GAGCGGAAGAAACGGACCG
	Reverse	CCTTAGGGTCTCCATTGAGCA
<b>Col3a1</b>	Forward	CCTGGCTCAAATGGCTCAC

	Reverse	CAGGACTGCCGTTATTCCCG
<b><i>Pparg2</i></b>	Forward	TCGCTGATGCACTGCCTATG
	Reverse	GAGAGGTCCACAGAGCTGATT
<b><i>Col7a1</i></b>	Forward	ACCACGTTTCTGACCGTGTC
	Reverse	AGCTGTGTCCACTAAATCTTGG
<b><i>Plin1</i></b>	Forward	CTGTGTGCAATGCCTATGAGA
	Reverse	CTGGAGGGTATTGAAGAGCCG
<b><i>Cxcl1</i></b>	Forward	CACCCGCTCGCTTCTCTG
	Reverse	TCTTGAGGTGAATCCCAGCC
<b><i>Col4a1</i></b>	Forward	TCCGGGAGAGATTGGTTTCC
	Reverse	CTGGCCTATAAGCCCTGGT



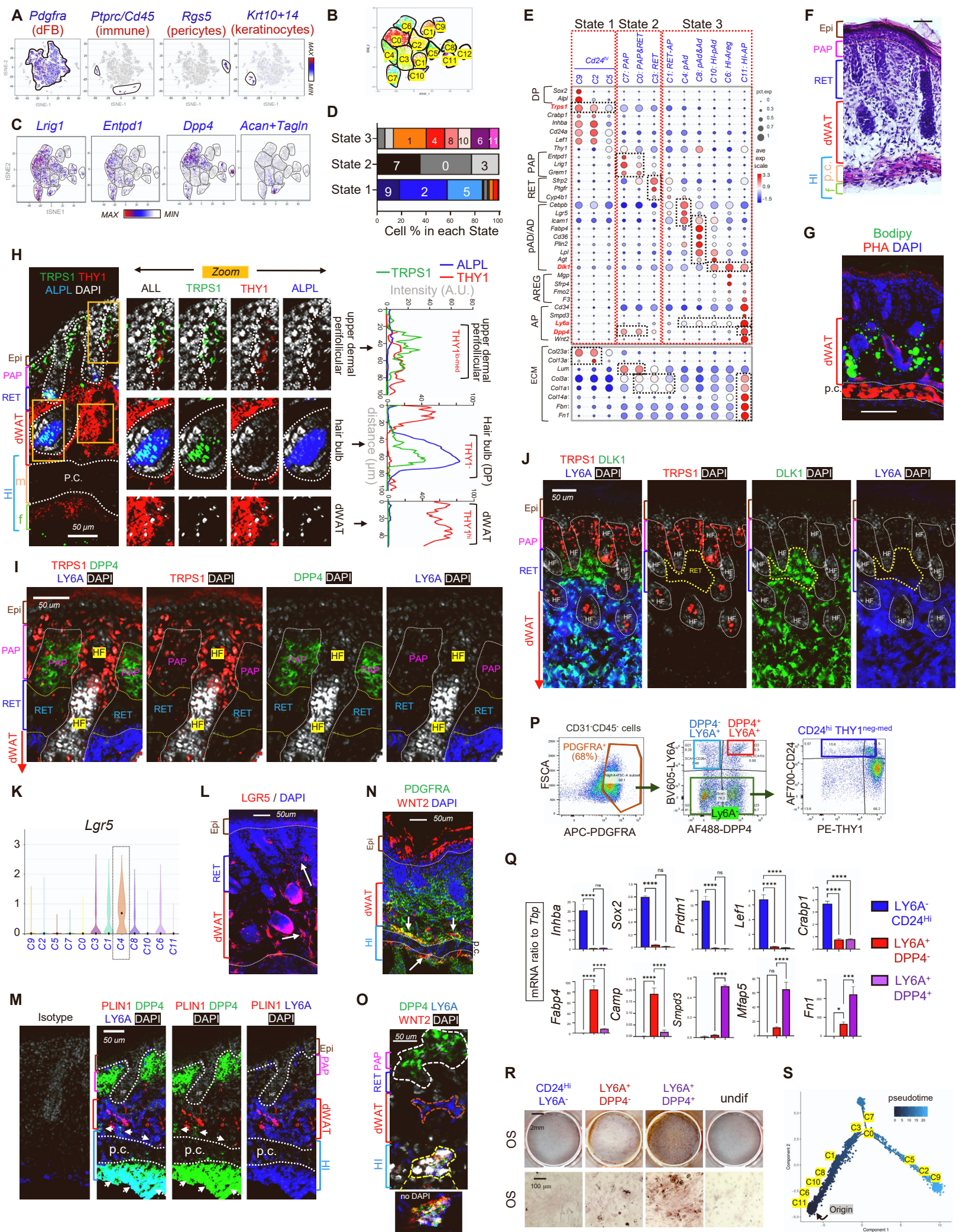


**Figure S1 (related to Figure 1). Characterization of heterogeneous dermal adipocyte lineage cells in developing neonatal skin**

(A) tSNE plots showing the expression of *Pdgfra*, *Ptprc/Cd45*, *Rgs5*, and *Krt10+Krt14* in neonatal mouse skin cell clusters.

(B-C) Neonatal mouse *Pdgfra*<sup>+</sup> dFBs were re-clustered into 13 clusters, and t-SNE plots for cell distribution by clusters (B) and indicated marker genes expression (C) were shown. Note that to focus on clusters related to adipogenesis, clusters including *Dpp4-Entpd1+Lrig1+* PAP dFB clusters and an *Acan+Tagln+* dermal sheath cluster were excluded from the rest of this study.

(D) Neonatal dFBs were grouped into 3 cell states by trajectory analysis with Monocle, and the percentage of clusters in each cell state is shown.

(E) Bubble plots of indicated genes in neonatal dFB clusters

(F) HE staining of neonatal skin sections. Scale bar, 50  $\mu$ m.

(G) Staining of neonatal skin sections with Bodipy (green dye for lipid) and phalloidin (red dye for actin fiber) staining

(H) Immunostaining of neonatal skin sections with TRPS1 (green), THY1 (red) and ALPL (blue), and DAPI was counterstained in white. White dotted line marks junction between the dermis and the epidermis or hair follicles. Scale bar, 50  $\mu$ m. The right panel is the quantified results showing the fluorescent intensity (arbitrary unit, AU) of TRPS1 (green), ALPL (blue), and THY1 (red) from top to bottom of the indicated zoomed images (representative of n=3/group).

(I-J) Immunostaining of neonatal skin sections with TRPS1 (red), LY6A (blue) and DPP4 (green) in I or DLK1 (green) in J, and DAPI in white. Dotted line marks junction between the papillary dermis, reticular dermis, and the epidermis or hair follicles. In J, a reticular dermal region (RET), that was TRPS1-DLK1<sup>+</sup>LY6A<sup>-</sup>, was circled by yellow dotted lines. Scale bar, 50  $\mu$ m. (K) Violin plot showing the expression of *Lgr5* across various *Pdgfra*<sup>+</sup> dFB clusters.

(K) Violin plot showing the expression of *Lgr5* across various *Pdgfra*<sup>+</sup> dFB clusters.

(L) Immunostaining of neonatal skin sections with LGR5 (red) and DAPI was counterstained in blue. Scale bar, 50  $\mu$ m. White arrows indicate LGR5<sup>+</sup> pAds in the reticular dermis or dWAT layer.

(M) Immunostaining of neonatal skin sections with PLIN1 (red), LY6A (blue) and DPP4 (green), and DAPI was counterstained in white. Arrows mark DPP4<sup>+</sup>LY6A<sup>+</sup> cells in the HI region above p.c. muscle. Scale bar, 50  $\mu$ m.

(N) Immunostaining of neonatal skin sections with WNT2 (red) and PDGFRA (green), and DAPI was counterstained in blue. Arrows mark WNT2<sup>+</sup>PDGFRA<sup>+</sup> cells in the HI region. Scale, 50  $\mu$ m.

(O) Immunostaining of neonatal skin sections with WNT2 (red), DPP4 (green) and LY6A (blue), and DAPI was counterstained in white. Scale bar, 50  $\mu$ m.

(P) Flow sorting strategies to sort various dFB sub-populations, including the perifollicular dFBs (CD24<sup>hi</sup>LY6A<sup>-</sup>), pAds (DPP4-LY6A<sup>+</sup>) and HI-APs (DPP4<sup>+</sup>LY6A<sup>+</sup>).

(Q) Sorted cells were subjected to qRT-PCR analysis of indicated dFB genes (n = 3 per group).

(R) Sorted cells were subjected to in vitro osteocyte differentiation assay, and osteocytes were stained with Alizarin Red (AR). Zoom-out images in the lower panel.

(S) Cell trajectory analysis of neonatal dFB clusters (C0~C11), and pseudotime (arbitrary units) is depicted from dark to light blue (left).

All error bars indicate mean  $\pm$  SEM. \*p < 0.05, \*\*p < 0.01, \*\*\*p < 0.001.

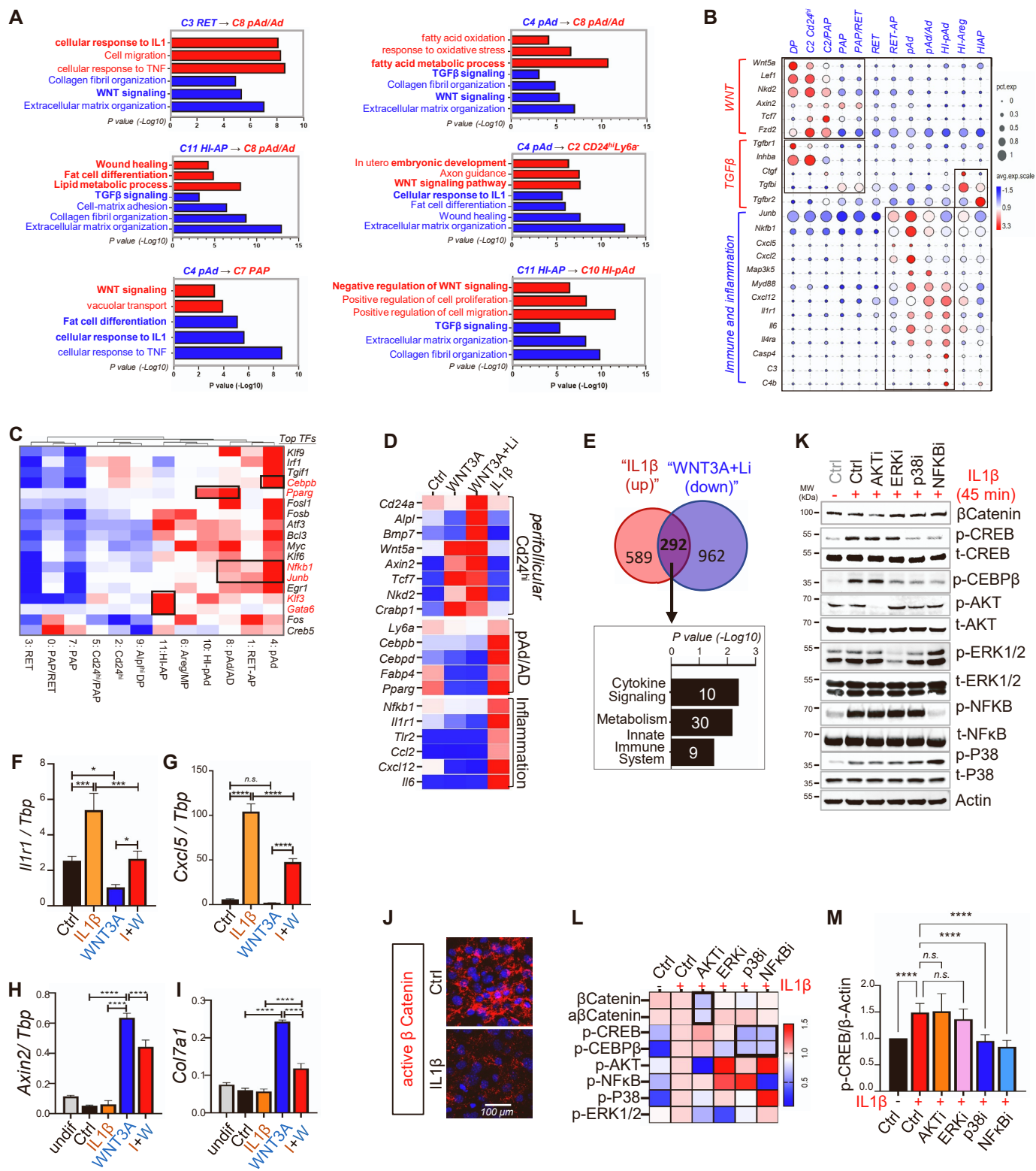


Figure S2

**Figure S2 (related to Figure 2) Interplay between the WNT- $\beta$ -catenin and IL1-immune signaling pathways during the conversion of dermal fibroblasts to adipocytes**

**(A)** KEGG/GO pathway analysis showing the top activated (red) or suppressed (blue) pathways during cell transition between indicated neonatal dFB clusters.

**(B)** Bubble plots showing the expression of indicated genes belonging to WNT, TGF $\beta$ , or immune/inflammation pathways across various neonatal dFB clusters.

**(C)** SCENIC analysis showing the top enriched transcriptional factors in neonatal dFB clusters.

**(D)** Neonatal dFBs were treated with WNT3A, Lithium, or IL1 $\beta$  for 48 hrs then subjected to bulk RNA-Seq. Heatmap showing mRNA expression of indicated genes.

**(E)** Venn diagram comparing genes up-regulated by IL1 $\beta$  and genes downregulated by WNT3A and lithium and top enriched pathways is shown in the lower panel.

**(F-I)** qRT-PCR analysis of the expression of indicated genes in neonatal dFBs treated with WNT3A and/or IL1 $\beta$  under undifferentiated condition (**F-G**) or adipocyte differentiation condition (**H-I**) (n=4/group).

**(J)** Neonatal dFBs were treated with IL1 $\beta$  for 48 hours then subjected to immunostaining analysis of active  $\beta$ -catenin (red) and DAPI (blue) (Scale bar, 100  $\mu$ m). Note that  $\beta$ -catenin, upon being phosphorylated by GSK3, is targeted to proteasome for degradation, and the active  $\beta$ -catenin antibody we used specifically recognized the non-phosphorylated form of  $\beta$ -catenin, which cannot be degraded.

**(K-M)** Neonatal dFBs were pretreated with specific inhibitors followed with stimulation with IL1 $\beta$  for 45 mins. Cell extracts were subjected to phospho-blotting analysis (**K**) using indicated antibodies and quantified results of heatmap are shown in **L** (average of n=3/group). Bar graph showing ratio of p-CREB / $\beta$ -Actin is shown in **M** (n=3/group).

All error bars indicate mean  $\pm$  SEM. \*p < 0.05, \*\*p < 0.01, \*\*\*p < 0.001.

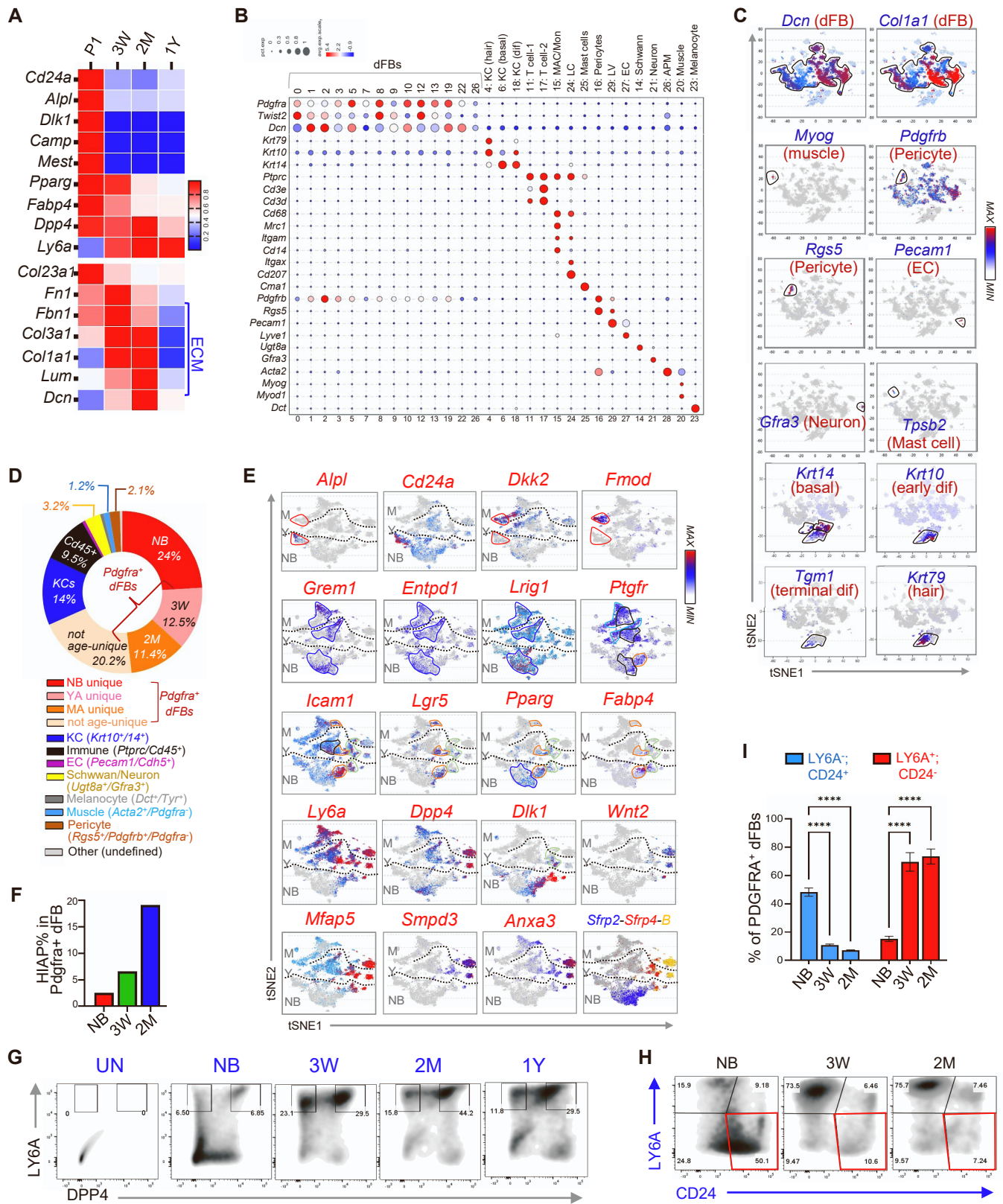


Figure S3

**Figure S3 (related to Figure 3). Tracing dermal adipogenesis and fibrogenesis during skin maturation.**

**(A)** Heatmap showing the mRNA expression kinetics (based on bulk RNAseq) of listed dFB/Ad marker or ECM genes in mouse skin at the indicated age.

**(B~C)** Bubble chart **(B)** and t-SNE plots **(C)** showing the expression of indicated marker genes in total skin cell clusters.

**(D)** Pie chart showing age-related changes in the percentage of various cell types, including *Pdgfra*<sup>+</sup> dFBs (68%), *Krt10/14*<sup>+</sup> keratinocytes (14%), *Ptprc/Cd45*<sup>+</sup> immune cells (9.5%), Schwann/neurons (3.2%), pericytes/vascular smooth muscle cells (VSMC, 2.1%), *Myog*<sup>+</sup> muscle cells (1.2%), melanocytes (0.7%), endothelial cells (EC, 0.6%), and arrector pili muscle (APM, 0.5%)

**(E)** t-SNE plots showing the expression of indicated marker genes in the reclustered *Pdgfra*<sup>+</sup> dFB clusters. Cells derived from different ages are separated with dotted lines. NB, newborn; Y, young (3 weeks of age); M, mature (2 months of age)

**(F)** Quantified percentage of HI-AP in indicated ages based on scRNA-seq (n=1/group).

**(G)** FACS plots showing the expression of DPP4 and LY6A in *CD31*<sup>-</sup>*CD45*<sup>-</sup>*PDGFRA*<sup>+</sup> dFBs (representative of n=3/group).

**(H-I)** FACS plots **(H)** showing the expression of LY6A and DPP4 in *CD31*<sup>-</sup>*CD45*<sup>-</sup>*PDGFRA*<sup>+</sup> dFBs, and quantified bar graphs of indicated cell population percentage are shown in **I** (n=3/group). All error bars indicate mean  $\pm$  SEM. \*p < 0.05, \*\*p < 0.01, \*\*\*p < 0.001.

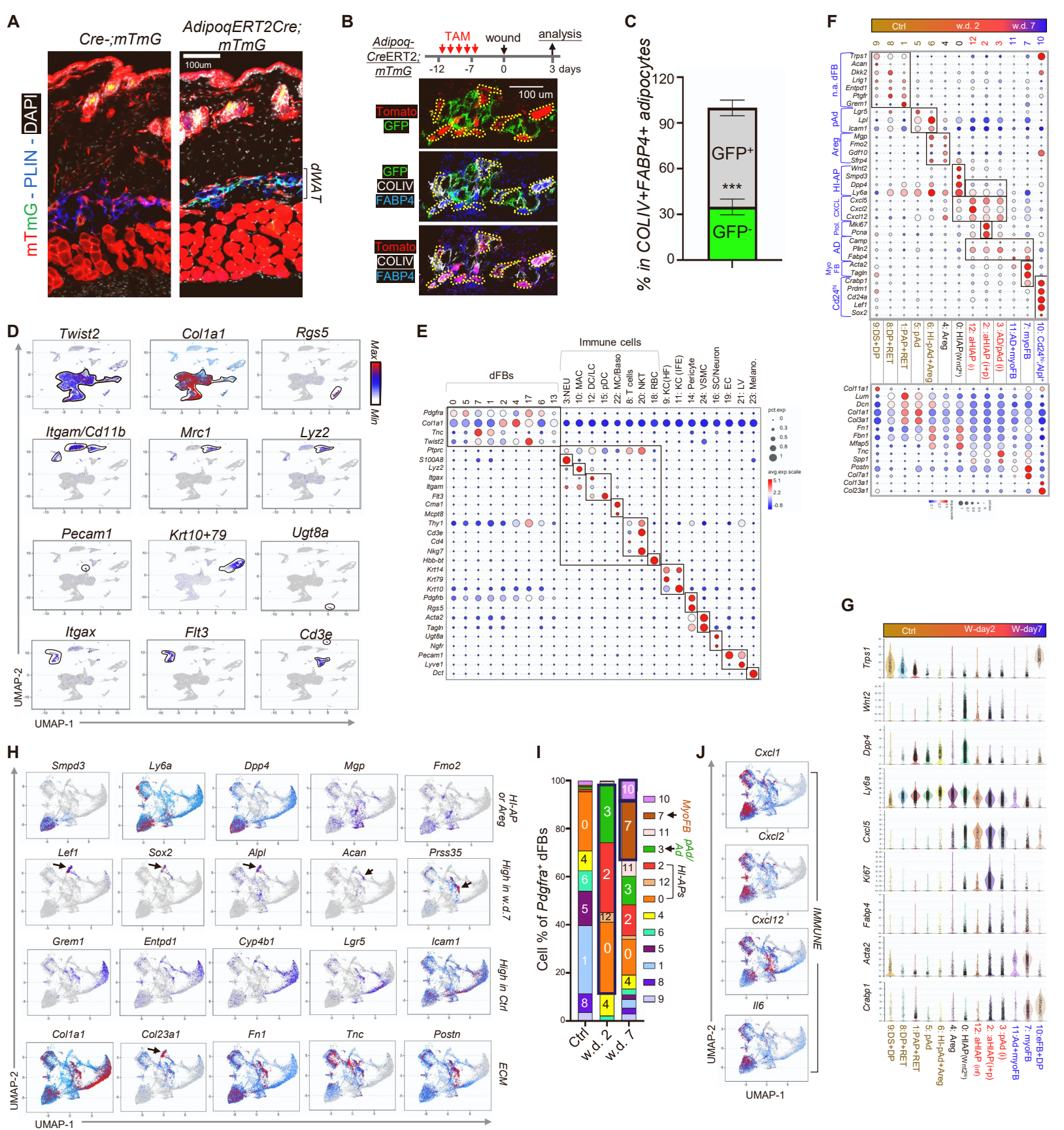


Figure S4

**Figure S4 (related to Figure 4) Tracing dermal adipogenesis and fibrogenesis during skin wound healing.**

**(A)** *Adipoq-CreERT2;mTmG* mice were administrated with tamoxifen (TAM) from day 12 ~ 7 prior to wounding, and unwounded control tissues were collected for immunostaining of COLIV (white), and GFP (green) and tomato (red) were overlaid to confirm that PLIN1<sup>+</sup> adipocytes were successfully labeled by GFP (representative of n=3/group). Scale bar, 100  $\mu$ m.

**(B)** *Adipoq-CreERT2;mTmG* mice were administrated with tamoxifen (TAM) from day 12 ~ 7 prior to wounding, and wound tissues were collected at w.d. 3 for immunostaining of COLIV (white), and GFP (green) and tomato (red) were overlaid. Scale bar, 100  $\mu$ m.

**(C)** Stacked bar graphs showing the quantification of the percentage of GFP<sup>+</sup> or GFP<sup>-</sup> cells in COLIV<sup>+</sup>FABP4<sup>+</sup> adipocytes as shown in **B** (n=3/group).

**(D-E)** W.d. 2, W.d. 7 and unwounded control skin samples were collected and subjected to scRNA-seq analysis. UMAP plot (**D**) or bubble chart (**E**) or showing the expression of indicated marker genes for each cluster.

**(F-J)** *Pdgfra*<sup>+</sup> dFBs were reclustered as shown in Fig. 4G. Bubble plots (**F**), violin plots (**G**), and UMAP plots (**H**) showing the expression of indicated marker genes. Stacked bar graph (**I**) showing the percentage of each dFB cluster in ctrl, w.d. 2 or w.d. 7 samples. UMAP plots showing the expression of inflammatory cytokines/chemokines are shown in **J**.

All error bars indicate mean  $\pm$  SEM. \*p < 0.05, \*\*p < 0.01, \*\*\*p < 0.001.



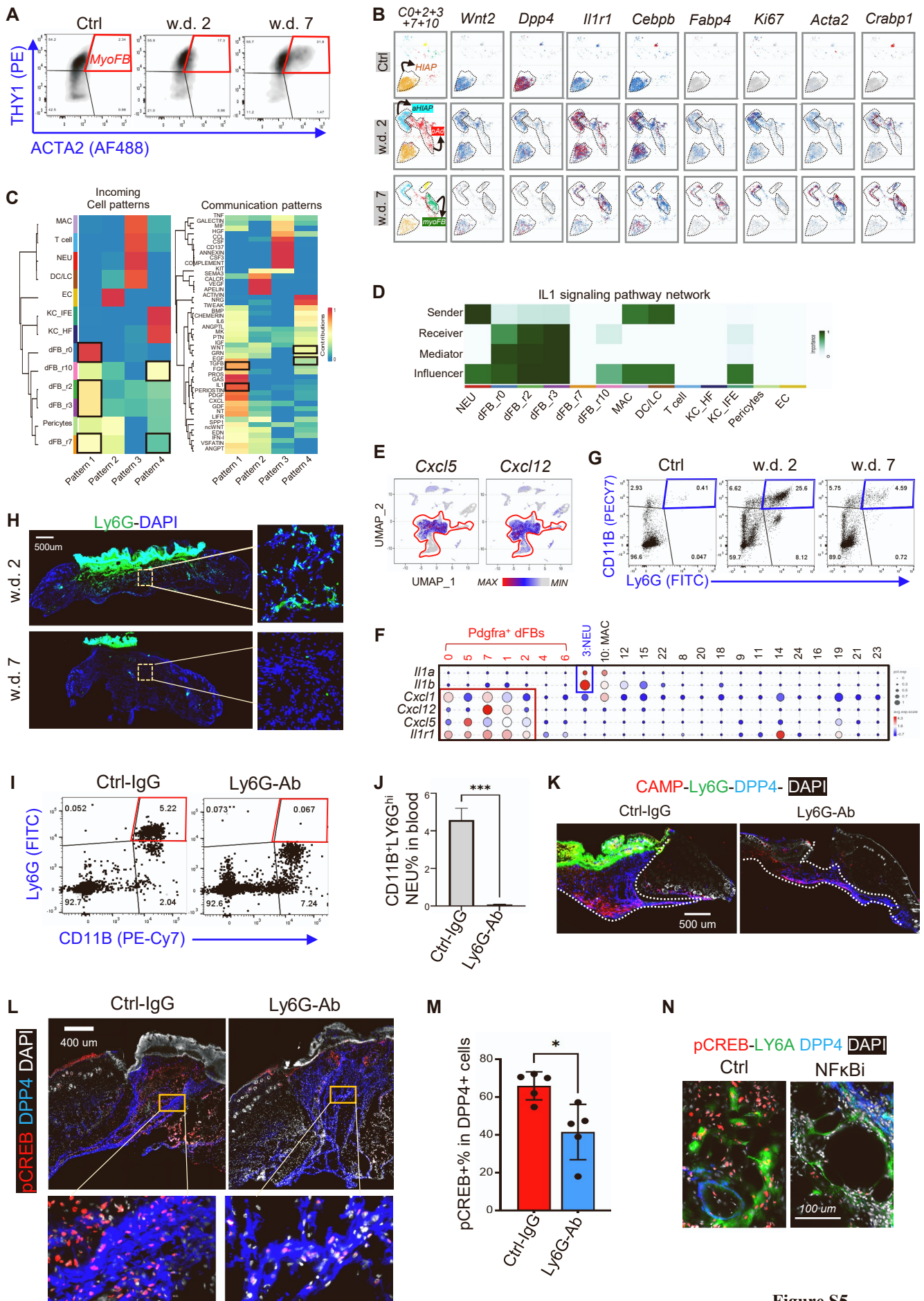
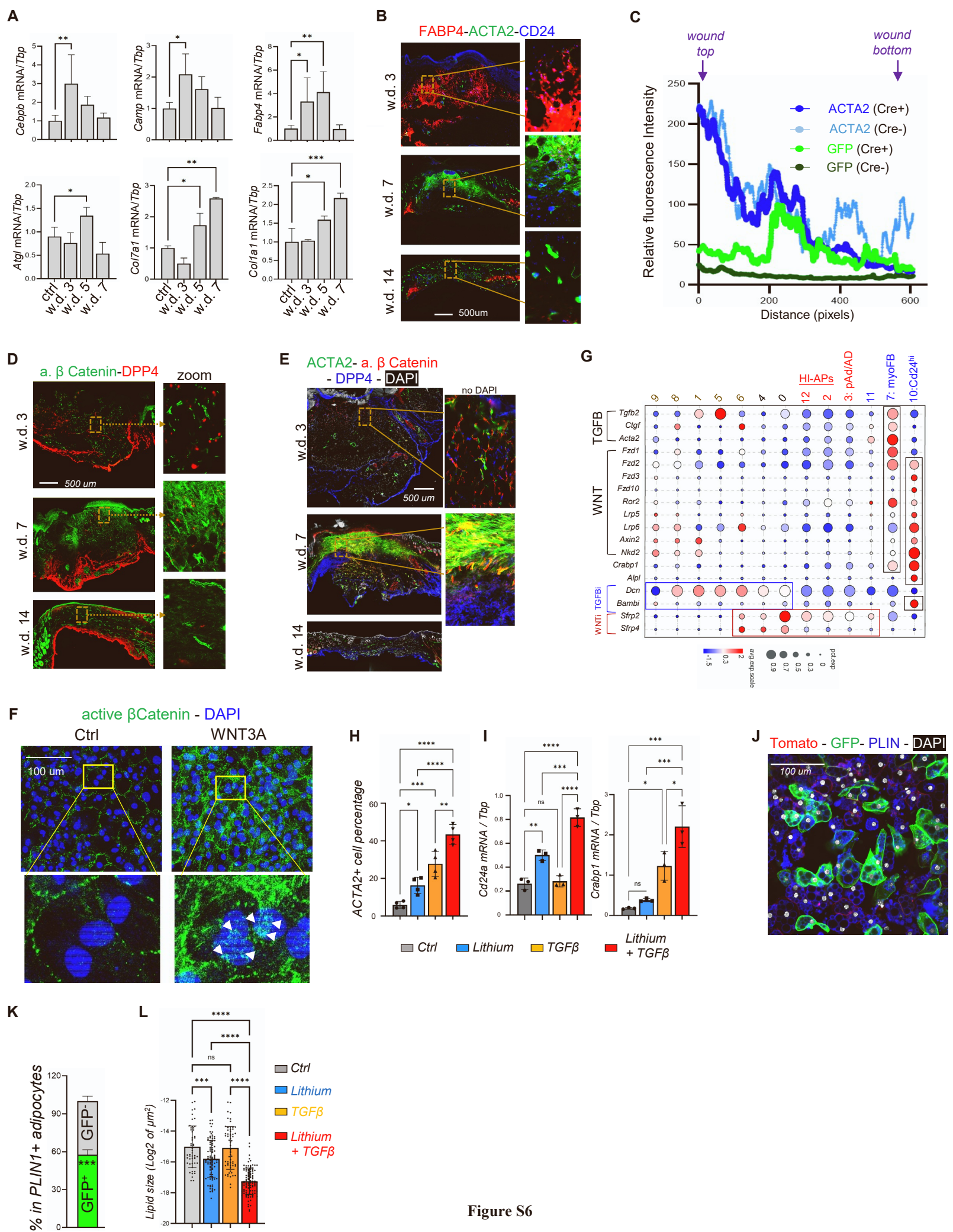


Figure S5

**Figure S5 (related to Figure 5). Wound-induced adipogenesis is regulated by neutrophils and the IL1 signaling axis.**

- (A) FACS plots showing THY1<sup>+</sup>SMA<sup>+</sup> myoFBs in control, w.d. 2 and w.d. 7 skin samples (representative of n=3/group).
- (B) UMAP plots showing how the expression of indicated genes were dynamically changed in C0, C2, C3, C7 and C10 dFB clusters during wound healing.
- (C) The inferred incoming communication patterns of skin cells showing the correspondence between the inferred latent patterns and cell groups and signaling molecules.
- (D) Heatmap showing the relative importance of each cell cluster as signal sender, receiver, mediator or influencer in IL1 $\beta$  signaling network.
- (E) tSNE plots showing the expression of *Cxcl5* and *Cxcl12* in all wound cell clusters.
- (F) Bubble plot showing the expression and/or distribution of indicated genes in all wound cell clusters.
- (G) FACS plots analyzing the presence of neutrophils (Ly6G<sup>+</sup>CD11B<sup>+</sup>) (representative of n=3/group).
- (H) Immunostaining of Ly6G (green) and DAPI (white) of w.d. 2 and w.d. 7 skin tissues. Scale bar, 500  $\mu$ m.
- (I-M) Mice were injected with isotype (ctrl) or anti-Ly6G antibodies to deplete neutrophils. FACS plots (I) and quantified bar graph (J) showing the presence of Ly6G<sup>+</sup>CD11B<sup>+</sup> neutrophils in blood samples from mice injected with ctrl-IgG or antiLy6G antibody (n=3/group). (K-M) Skin wounds were collected at w.d. 3. for immunostaining of CAMP (red), Ly6G (green) and DPP4(blue) (K), or pCREB (red) and DPP4 (blue) (L). Nuclei were stained with DAPI (white). Scale bar, 400  $\mu$ m. (M). Bar graphs showing quantified percentage of pCREB<sup>+</sup> cells in DPP4<sup>+</sup> cells (n=5/group).
- (N) Mice were injected *i.p.* with DMSO (ctrl) or NF- $\kappa$ B inhibitor and skin wounds were collected for immunostaining of pCREB (red), LY6A (green) and DPP4 (blue). Scale bar, 100  $\mu$ m.
- All error bars indicate mean  $\pm$  SEM. \*p < 0.05, \*\*p < 0.01, \*\*\*p < 0.001.



**Figure S6 (related to Figure 6) Activation of WNT and TGF $\beta$  signaling pathways in adipocyte lineage cells during the wound-proliferative phase.**

(A) Bar graphs showing the mRNA expression kinetics of listed genes during skin wound healing (n=3 per group). All error bars indicate mean  $\pm$  SEM. \*p < 0.05, \*\*p < 0.01, \*\*\*p < 0.001.

(B) Mouse wound tissues were immuno-stained with indicated antibodies. Scale bar, 500  $\mu$ m.

(C) Quantified intensity profiles of Fig.6B image showing signals from ACTA2 or GFP in Cre- or Cre+ wounds from wound top to bottom (representative of n=3/group).

**Supplemental result for Fig. S6C:** Indeed, ACTA2<sup>+</sup>GFP<sup>-</sup> myofibroblasts were also detected in the wound, indicating that myofibroblasts can also be derived from other cell types, such as papillary and reticular fibroblasts, HI-APs and preadipocytes that do not express Adipoq.

(D-E) Wound tissues were stained with active  $\beta$ -catenin, ACTA2 and/or DPP4 as indicated. Scale bar, 500  $\mu$ m.

(F) Primary dFBs were treated with WNT3A (10ng/mL) or vehicle control for 24 hrs, and cells were collected for immunostaining analysis with active  $\beta$ -catenin antibody (green), and nuclei were counterstained with DAPI (blue).

However, it is difficult to distinguish  $\beta$ -catenin within nuclei from that within the cytosol in cells that are tightly packed within whole wound tissue. Note that clear nuclear signal of  $\beta$ -Catenin could be detected in cultured primary dFBs stimulated with WNT ligand, although the majority of active  $\beta$ -Catenin was retained in the cytosol or membrane (Fig. S6F).

(G) Bubble plots showing the expression of indicated genes across various dFB clusters shown in Fig. 4G-H. **Supplemental results for Fig. S6G:** Interestingly, we found that all dFB clusters, except the r7 and r10 dFBs, expressed several TGF $\beta$  and/or WNT pathway inhibitor genes (Fig. S6G), which may dampen the responsiveness of these cells to external TGF $\beta$  and/or WNT signaling.

(H-I) Differentiated mature adipocytes were treated with Lithium  $\pm$  TGF $\beta$ 2 as shown in Fig. 6E. (H) quantification of the percentage of ACTA2<sup>+</sup> cells (n=4/group). (I) qRT-PCR analyses of the expression of indicated genes (n=3/group).

(J-L) Mature adipocytes were differentiated from dFBs isolated from *Adipoq-CreERT2;mTmG* mice in the presence of tamoxifen.

(J) Cells were immunostained with PLIN1 (blue) to determine the efficiency of the genetic labeling of PLIN1<sup>+</sup> adipocytes by GFP. Scale bar, 100  $\mu$ m. (K) Stacked bar graphs showing the quantification of the percentage of GFP<sup>+</sup> or GFP<sup>-</sup> cells in PLIN1<sup>+</sup> adipocytes (n=3/group). (L) Bar graph showing the quantification of changes in lipid droplet size as shown in Fig. 6I (LD quantified from n=5 fields/group).

**Results for J-K:** Approximately 60% of the differentiated PLIN1<sup>+</sup> adipocytes were successfully labeled with membrane-bound GFP.

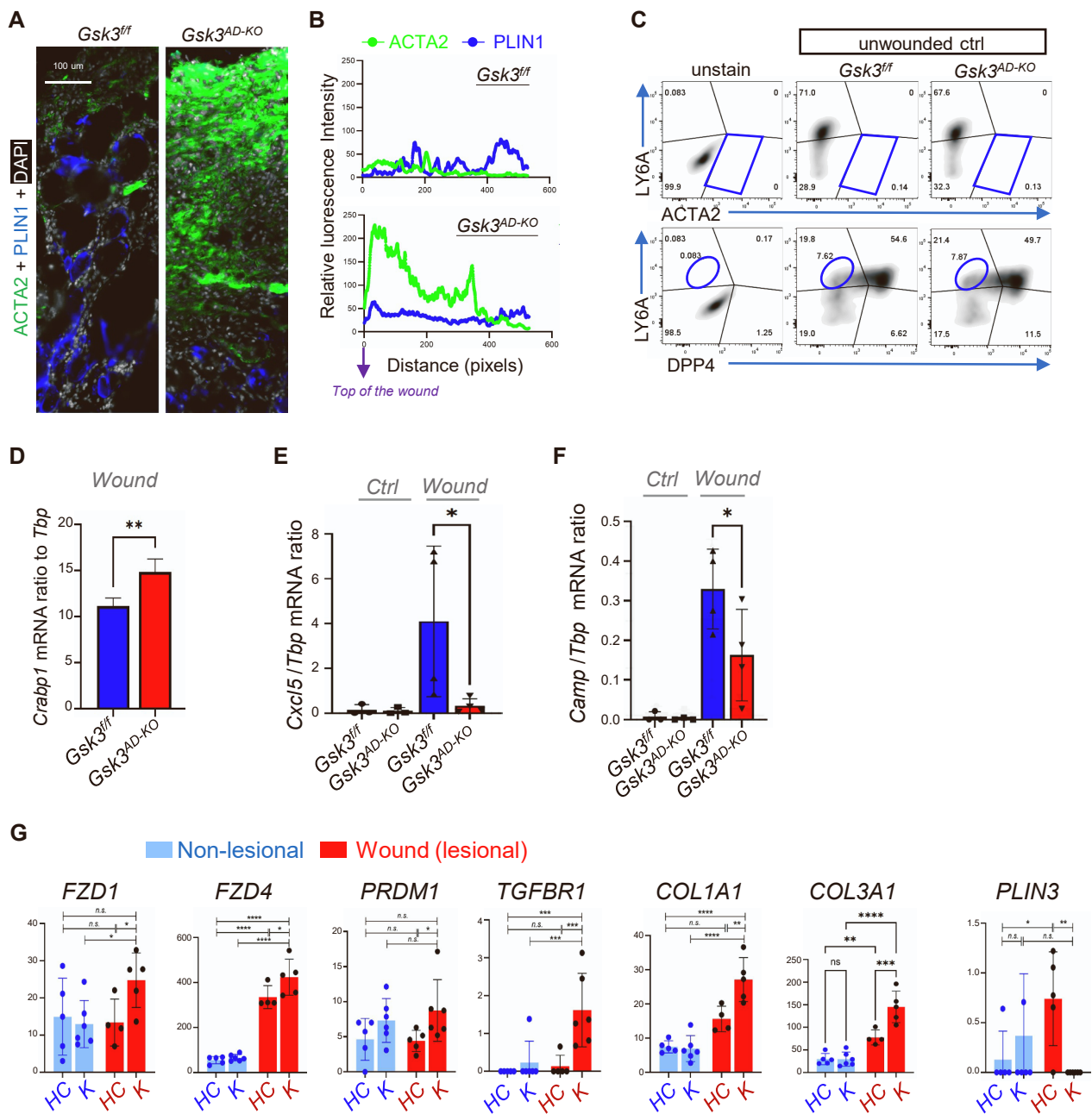


**Figure S7 (related to Figure 7) WNT activation in adipocytes promotes myfibroblast formation during wound healing.**

(A-B) Skin wound tissues (w.d. 7) were collected from wildtype control (*Gsk3<sup>fl/fl</sup>*) or *Gsk3* adipocyte conditional knockout (*Adipoq-CreERT2;Gsk3<sup>fl/fl</sup>*) mice. (A) Wound tissues were stained with ACTA2 (green) and DPP4 (blue), and DAPI in white. Scale bar, 100  $\mu$ m. (B) Quantified intensity profiles of Fig.S6A showing signals from all three fluorescent channels from wound top to bottom (representative of  $n=3$ /group).

(C-F) Unstained control or ununwounded control FACS plots for Fig. 7E showing the percentage of ACTA2<sup>+</sup>LY6A<sup>+</sup> myfibroblasts or LY6A<sup>+</sup>DPP4<sup>-</sup> in PDGFRA<sup>+</sup> dFBs (representative of  $n=3$ /group). (D) qRT-PCR analyses showing the mRNA expression of *Crabp1* in the wound granular tissues ( $n=3$ /group). (E-F) qRT-PCR analysis of *Cxcl5* (E) and *Camp* (F) ( $n=3$ /group).

(G) Bar graphs showing relative mRNA expression (based on RNA-seq FPKM values) of listed genes in non-lesional and wound tissues from health control (HC) or keloid (K) individuals ( $n=4\sim5$ /group).

All error bars indicate mean  $\pm$  SEM. \* $p < 0.05$ , \*\* $p < 0.01$ , \*\*\* $p < 0.001$ .